

**2000 Technical Meeting**  
**of**  
**Central States Section**  
**The Combustion Institute**

**Combustion**  
**Fundamentals and Applications**

**Proceedings Editor, Papers Chair,**  
**D. L. Reuss, General Motors R & D Center**

**Program Chair**  
**C. S. Daw, Oakridge National Laboratories**

**Local Arrangements**  
**J. P. Gore and S. H. Frankel, Purdue University**  
**N. Rizk, Rolls Royce Allison Engine Company**

**April 16 - 18, 2000: Hyatt Regency Hotel, Indianapolis, Indiana, USA**

# Mine Fire Source Discrimination Using Fire Sensors and Neural Network Analysis

J.C. Edwards\*, G.F. Friel, R.A. Franks, C.P. Lazzara, and J.J. Opferman  
National Institute for Occupational Safety and Health  
Pittsburgh Research Laboratory  
Pittsburgh, PA 15236

## Abstract

Fire experiments were conducted in the Safety Research Coal Mine (SRCM) at the National Institute for Occupational Safety and Health, Pittsburgh Research Laboratory, with coal, diesel-fuel, electrical-cable, conveyor-belt, and metal-cutting fire sources to determine the response of fire sensors to products-of-combustion (POC). Metal oxide semiconductor (MOS) and smoke fire sensors demonstrated an earlier fire detection capability than a CO sensor. This capability was of particular significance for a conveyor-belt fire in which the optical visibility was reduced to 1.52 m with an increase in CO of less than 2 ppm at a distance of 148 m from the fire. Application of a neural-network program to the sensor responses from each type of fire source resulted in correct classifications of coal, diesel-fuel, cable, belt, and metal-cutting combustion with a mean of 96% of the test data correctly classified.

## Introduction

Fire detection in underground coal mines is important for early fire location and safe miner evacuation. Fire detection is aided by the in-mine ventilation which transports the fire products-of-combustion (POC) from the fire source to fire sensors, and it is impeded by the diluting effects of the ventilation which reduces the measurable signal. Early mine fire detection experiments in both normally ventilated and near zero airflow mine entries have been previously investigated experimentally [1, 2]. The results of that research showed the improved performance of ionization and optical smoke fire sensors over CO sensors. The next advancement beyond early detection, in addition to determination of the fire location, is the determination of the material burning, the mode of combustion, and the extent of fire growth. This knowledge can be applied to the determination of appropriate actions to be taken to extinguish a mine fire and to initiate escape and rescue procedures for miners. Various in-mine materials can provide the initial fuel for a mine fire. The common fire source materials considered in this program were coal, diesel fuel, electrical cable, conveyor belt, and acetylene gas used for metal cutting. The solid material combustion was advanced using heaters through a smoldering combustion stage to produce a slowly increasing range of measurable POC. The POC include

CO and other oxidizable gases and smoke particles with submicron diameters.

It is the types of combustion products and their rate of change which will indicate the combustion material, mode, and growth rate. One method which can be deployed to make these determinations is the use of multiple fire sensors to discriminate the POC. The rapid analysis of mine fire products with a neural network program has been reported elsewhere [3, 4]. These approaches utilize temperature and gaseous POC from combustion of home materials [3] and laboratory heating of coal [4]. CO and smoke sensors are used for the early detection of underground coal mine fires. While CO sensors, in the absence of cross-interference from other gases, respond to the concentration of CO, the response of smoke sensors in mining applications is presented in terms of the smoke optical density. Ultimately, the optical density depends upon the smoke mass concentration, smoke particle diameter, and the dielectric constant of the smoke particles. Ionization smoke sensors are more responsive to smoke from flaming combustion, and optical smoke sensors are more responsive to smoke from smoldering combustion. The intense turbulent combustion during the flaming stage reduces the average particle size associated with smoldering combustion.

In addition to these fire sensors, there are MOS sensors

---

\*Corresponding author: [jce9@cdc.gov](mailto:jce9@cdc.gov)

Proceedings of the 2000 Technical Meeting of the Central States Section of the Combustion Institute

which respond to oxidizable gases. These MOS sensors operate on the principle that oxygen ( $O_2$ ) is adsorbed on the surface at grain boundaries which increases the electrical resistance across the surface. The oxidation of POC gases removes  $O_2$  from the surface and reduces the electrical resistance across the surface. The measurable change in surface resistance is a measure of the POC concentration. These sensors are very responsive but not very selective of the target gas. They are also temperature and humidity dependent. However, it is their extreme sensitivity to various hydrocarbons that increases their potential for use as mine fire sensors. The selection of a base set of multiple sensors is a key decision for a neural network program to successfully discriminate between hazardous mine-fire combustion and normal mining combustion that may result from sources such as diesel engines and cutting and welding procedures.

### Specific Objectives

This research has two objectives. One objective is to evaluate the comparative time sequence of alarm values for CO, smoke, and MOS fire sensors for in-mine combustible source fires. The second objective is to determine a suitable set of mine fire sensors and a neural network analysis program which can be used to classify a mine fire combustible source.

### Experimental Method

The plan view of the SRCM section in which the experiments were conducted is shown in figure 1.

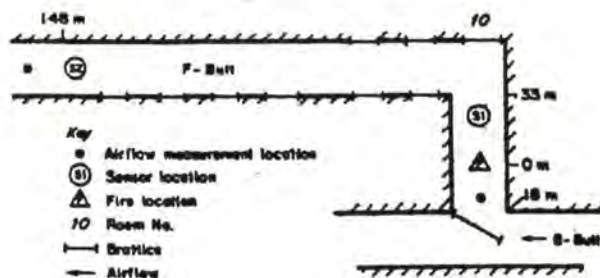


Figure 1. Plan view of mine section.

Room 10, in which the fire is located, has an average height and width of 2.0 m and 3.9 m, respectively. F-Butt has an average height and width of 1.9 m and 4.5 m, respectively. The cloth brattice at Room 10 and B-Butt was adjusted to regulate the airflow into Room 10 and F-Butt. Air quantity measurements were made at the fire zone and near the end of F-Butt, 7.6 m downwind from sensor station S2. For the experiments conducted, the average air

quantity at the fire zone was 3.49  $m^3/s$  and at the end of F-Butt was 5.17  $m^3/s$ . The increase in air quantity downwind of the fire zone was caused by air leakage into F-Butt around brattices shown along the ribs in figure 1 blocking crosscuts connecting F-Butt and parallel airways. The fire sensors used for the experiments are listed in table 1 below.

Table 1. Fire sensor types used

Sensor	Type
SA	Optical Smoke
SB	Ionization Smoke
CO	Carbon Monoxide
FA, FB	MOS

Sensor SA is an optical path sensor which operates at an infrared wavelength with a transmitter-receiver separation path of 9.65 m. Sensors SB, CO, FA, and FB are point-type sensors. Sensors FA and FB are MOS sensors which are similar in their responses to various POC gases. These sensors were located at station S2, as was an optical-path light monitor to measure the optical density of the smoke. At station S1, a CO sensor was located to calculate the transport time of the CO component of the POC between stations S1 and S2.

The heating of the coal, cable, and belt was conducted with electrical heaters to which power was supplied slowly such that the smoldering mode passed through a slow growth phase with the emanation of POC prior to flaming combustion in order to validate the sensitivity of the fire sensors and to duplicate a slowly developing mine-fire event. The heating time prior to flaming combustion for the solid fuels varied between 42 and 109 min. To validate the discriminating capability of a neural network program when applied to a normal mine combustion source, an experiment was conducted which consisted of cutting a rail section with an acetylene torch 14 m upwind from sensor station S2.

### Neural Network Analysis

A neural network analysis was applied to the classification of fire sensor responses to differentiate between possible fire events. In this neural network, temporal experimental data were compared to the nonlinear approximations generated by the neural network until adequate approximations for correct classifications were obtained through corrective iterations. The input layer of neurons contained the experimental sensor data along with variables generated from the experimental data. The output layer of neurons contained the fire source classifications generated by the neural network. Between the input and output layers were two hidden layers of

neurons or process elements (PEs). The inputs to the hidden layers of neurons were multiplied by weights, summed, and processed through a bounded, nonlinear activation function. In the training phase of the neural network, the output classifications were subtracted from the correct classifications and the differences, or errors, were used by a backpropagation method, which is a modification of the gradient-descent search technique, to adjust the values of the weights until a sum of the errors was less than a reasonable tolerance. For the sensor data analysis considered here, the neural network software package entitled NeuroSolutions for Excel™ from NeuroDimension, Inc. was used.

### Results and Discussion

Table 2 lists the fire experiments conducted with reference to fuel type and the relative alarm times of the fire sensors with respect to the sensor which alarmed first (indicated by 0 s). The estimated arrival time of the POC at station S2 from the flaming-stage, solid fuels, relative to the first sensor alarm time, is listed as  $T_f$  and is based upon the measured ventilation rate.

Table 2. Fire sensor relative alarm times

Exp.	Fuel	FA, s	FB, s	CO, s	SA, s	SB, s	$T_f$ , s
1	Coal	80	0	3521	556	736	1579
2	Diesel	34	0	105	6	34	na <sub>1</sub> <sup>1</sup>
3	Cable	219	59	2614	0	149	2388
4	Belt1	178	98	1486	38	0	1307
5	Coal	218	204	1590	0	242	881
6	Coal	174	0	3690	1736	2166	3242
7	Diesel	na <sub>3</sub> <sup>3</sup>	55	83	0	29	na <sub>1</sub> <sup>1</sup>
8	Diesel	0	7	196	42	84	na <sub>1</sub> <sup>1</sup>
9	Cable	149	109	2746	0	191	2518
10	Belt1	952	892	2709	0	294	2572
11	Belt2	14	0	2853	156	92	na <sub>2</sub> <sup>2</sup>
12	Belt3	910	758	4735	406	0	4627

<sup>1</sup>Symbol na<sub>1</sub> - flame at initial heating time.

<sup>2</sup>Symbol na<sub>2</sub> - no flaming combustion.

<sup>3</sup>Symbol na<sub>3</sub> - alarm not achieved due to fuel vapors.

\*\*Reference to a specific product does not imply endorsement by NIOSH.

The alarm time for CO is based upon a 5-ppm rise above the ambient concentration. For the smoke and MOS sensors, the alarm time is based upon a ten-standard-deviation change from the sensor ambient signal. A ten-standard-deviation change is less probable than a value at the mean in a Gaussian distribution by a factor of about  $10^{-22}$ . The diesel fuel experiments required the calculation of a background value for sensors FA and FB which excluded vapors from heptane used to ignite the fuel. In the case of experiment No. 7, the background concentration was too high to define an alarm for FA. Table 2 shows that the smoke and MOS fire sensors always alarmed before the solid fuel, flaming-stage POC reached the sensor station at time  $T_f$ , which occurred before the CO sensor alarm time. For the diesel fuel fires, the smoke and MOS fire sensors alarmed prior to the CO sensor. Figure 2 shows for

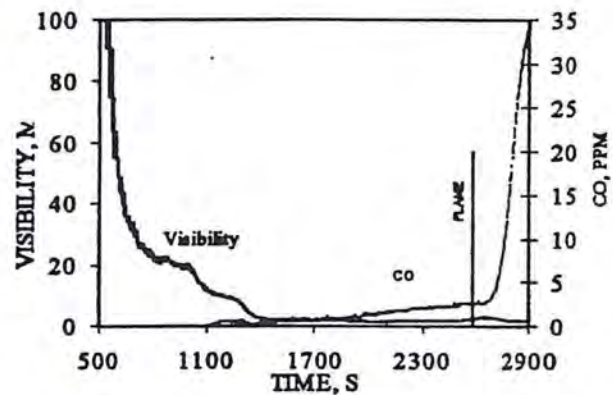


Figure 2. Visibility and CO concentration at station S2 for experiment No. 10.

experiment No. 10 that the optical visibility, which is calculated from the optical density measured by the light obscuration monitor as defined by a visibility optical density relationship [5], decreased to 1.52 m while the CO concentration increased to 1.1 ppm above ambient concentration 1,900 s after the first alarm and, based upon table 2 data, 948 s after the last of the non-CO, fire-sensor alarms. A visibility of 36.4 m corresponds to an optical density of  $0.022 \text{ m}^{-1}$ , which is the alarm value for a mine-fire smoke sensor. The times plotted in figure 2 are from the first alarm time. The flaming mode POC did not reach the sensor station until 2,572 s after the first sensor alarmed. This flaming event is coincidental with the significant increase in measurable CO seen in figure 2. The in-mine hazard of severely reduced visibility without a CO alarm, but with an alarm for each smoke sensor, reinforces the importance of fire smoke sensors.

In order to use the neural network program, the data for each experiment were prepared in files with the fire sensor signals normalized to their ambient background signals. For sensors FA and FB, the sensor electrical resistance

value was normalized to unity under ambient conditions. Figures 3 and 4 show the data recorded from coal fire experiment No. 6 for sensors FA, SA, SB, and the CO sensor relative to the first alarm time. The responses of FA and FB were nearly identical.

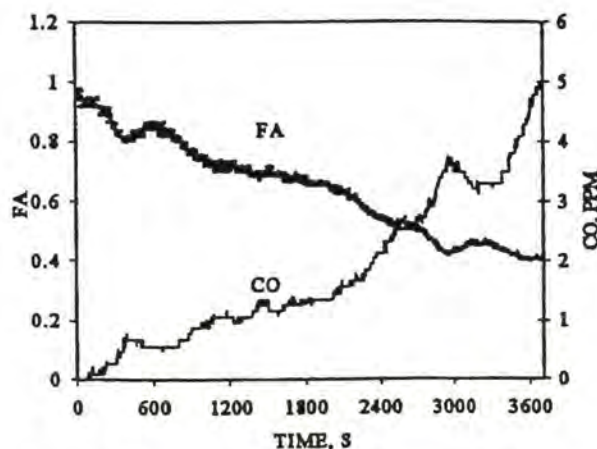


Figure 3. Sensors FA and CO response to coal combustion for experiment No. 6.

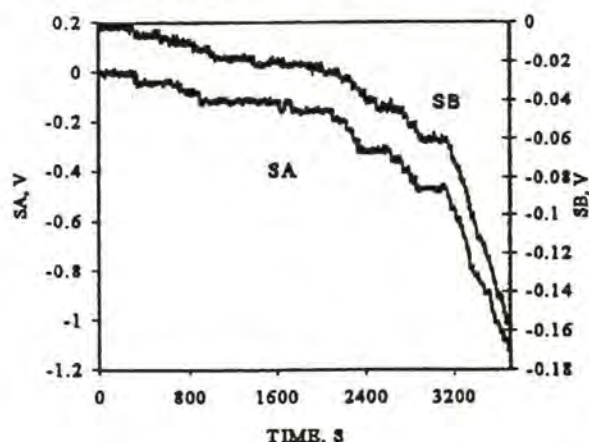


Figure 4. Sensor SA and SB response to coal combustion for experiment No. 6.

The training of the neural network was accomplished with the five sets of sensor data from coal, diesel-fuel, electrical-cable, and conveyor-belt fires, which are the fires of experiment numbers 1 to 4 in table 2, and an acetylene-torch, metal-cutting experiment. Seven data inputs were processed from the sensor data to classify the five fire types.

The inputs, which include time and multiplicative combinations of the data from four of the sensors but excluding sensor SB, were determined by trial-and-error to be the most suitable inputs for accurate classifications. The size of the training data sets ranged from 85 to 991

exemplars, or time samples, of the four sensor inputs and two functions of the sensor inputs with the total size of the training set being 2,988 exemplars. Time zero at the beginning of each data set corresponded to the first sensor alarm for each type of fire. Sampling by the sensors occurred at two-second intervals.

Various neural network programs provided in the package by the vendor were applied to the data in attempts to successfully classify the fire types. A two-hidden-layered perceptron network with momentum backpropagation of error algorithm produced reproducible results. No smoothing of the data or inclusion of rates of data change was necessary for successful training and testing. The first hidden layer consisted of 20 PEs and the second hidden layer consisted of 10 PEs. It was discovered that the testing results were reproducible even though the initial weights between the PEs were assigned randomly. The activation function used in the hidden layers was the hyperbolic tangent function with the output layer using a softmax classification function. One thousand epochs, or iterations, through the samples were performed with error correction after every epoch. The minimum squared error achieved after 1,000 epochs was 0.0012.

For testing the neural network, seven data files were presented to the trained network. These files included experiment numbers 5 to 10 in table 2 and 1 metal-cutting experiment. The number of testing exemplars in each file ranged from 121 to 1,854 with the total size of the testing set being 4,255 exemplars. Two coal and two diesel-fuel fires were included in the set of testing files. The percentage of exemplars predicted correctly in each of the seven testing data files is presented in table 3.

Table 3. Percentages of testing files predicted correctly

Exp.	5	6	7	8	9	10	Cutting
% Correct	100	86	90	99	94	100	100

The average correct classification of the seven tests in table 3 is 96%. The minimum value of 86% for a single experiment is not unreasonable. Evaluation of experiments 11 and 12 could not be made with the neural network program because experiments using materials similar to those of BELT2 and BELT3 were not available to include in the testing set.

### Conclusions

The role for mine-fire smoke sensors and MOS sensors was shown to be enhanced by their earlier alarm times relative to a CO sensor. The low optical visibility in the absence of significant CO for flammable material, BELT1, further supports the role of smoke sensors for early mine-fire detection. Data, recorded from an optical path smoke,

a CO, and MOS sensors placed in a multiple sensor arrangement and inserted into a backpropagation neural network program, enabled the program to correctly classify coal, diesel-fuel, electrical-cable, and conveyor-belt test fires and a metal-cutting procedure based upon a training set similar to the testing set. This correct mine fire combustible source classification is based upon an average 96% correct classification of seven tests of the test data with the worst case probability of a correct prediction being 86%.

#### Acknowledgements

The authors acknowledge the miners who maintain the Safety Research Coal Mine at the Pittsburgh Research Laboratory for their assistance in preparation of the experiments.

#### References

1. Edwards, J.C., Franks, R.A., Friel, G.F., Lazzara, C.P., and Opferman, J.J. *8th U.S. Mine Ventilation Symposium*, Univ. of Missouri-Rolla, (Univ. of Missouri-Rolla Press, Rolla, MO), pp. 295-301, (June 1999).
2. Edwards, J.C., Friel, G.F., Franks, R.A., and Opferman, J.J. *6th International Mine Ventilation Congress*, Pittsburgh, PA, (Society for Mining, Metallurgy, and Exploration, Littleton, CO), pp. 331-336, (May 1997).
3. Ishii, H. and Ono, T. *Fire Safety Science-Proceedings of the 4th International Symposium*, pp. 761-772, (1994).
4. Brinn, M. and Bott, B. *Mining Engineer* (London), v. 154, n. 396, pp. 71-74, (September 1994).
5. Rashash, D.J. *Fire International*, 2, n. 4, pp. 30-49, (1975).